

Therapeutic activation of macrophages and microglia to suppress brain tumor-initiating cells

Susobhan Sarkar^{1,2}, Axinia Döring^{1,2,6}, Franz J Zemp^{3,6}, Claudia Silva^{1,2}, Xueqing Lun³, Xiuling Wang³, John Kelly^{1,2}, Walter Hader^{1,2}, Mark Hamilton^{1,2}, Philippe Mercier^{1,2}, Jeff F Dunn², Dave Kinniburgh⁴, Nico van Rooijen⁵, Stephen Robbins³, Peter Forsyth³, Gregory Cairncross^{1,3}, Samuel Weiss² & V Wee Yong^{1,2}

¹Department of Clinical Neurosciences, University of Calgary, Calgary, Alberta, Canada.

²Hotchkiss Brain Institute, University of Calgary, Calgary, Alberta, Canada.

³The Southern Alberta Cancer Research Institute, University of Calgary, Calgary, Alberta, Canada.

⁴Centre for Toxicology, University of Calgary, Calgary, Alberta,

Canada. ⁵Department of Molecular Cell Biology, Vrije Universiteit, Amsterdam, The Netherlands.

⁶These authors contributed equally to this work. Correspondence

should be addressed to V.W.Y. (vyong@ucalgary.ca).

Brain tumor initiating cells (BTICs) contribute to the genesis and recurrence of gliomas. We examined whether the microglia and macrophages that are abundant in gliomas alter BTIC growth. We found that microglia derived from non-glioma human subjects markedly mitigated the sphere-forming capacity of glioma patient-derived BTICs in culture by inducing the expression of genes that control cell cycle arrest and differentiation. This sphere-reducing effect was mimicked by macrophages, but not by neurons or astrocytes. Using a drug screen, we validated amphotericin B (AmpB) as an activator of monocytoïd cells and found that AmpB enhanced the microglial reduction of BTIC spheres. In mice harboring intracranial mouse or patient-derived BTICs, daily systemic treatment with non-toxic doses of AmpB substantially prolonged life. Notably, microglia and monocytes cultured from glioma patients were inefficient at reducing the sphere-forming capacity of autologous BTICs, but this was rectified by AmpB. These results provide new insights into the treatment of gliomas.

Gliomas are the most common primary tumors that arise in the CNS in adults. The most malignant form, glioblastoma, is resistant to current modalities of treatment and has one of the worst 5-year survival rates of all human cancers. The neoplastic growth of malignant gliomas is thought to be maintained by a rare population of stem-like transformed cells that undergo self-renewal, BTICs. BTICs recapitulate glioma growth when implanted into the brains of immuno-compromised mice¹. Previously, we observed that as few as ten BTICs deposited into the striatum of NOD-SCID mice were sufficient to form intracranial tumors². In addition to their stem-like extensive potential to proliferate, BTICs contribute to the intractability of malignant gliomas by being relatively resistant to radiation³ and a variety of chemotherapeutic agents⁴, in contrast with their more differentiated transformed progenies. Recently, BTICs were found to account for glioma recurrence following efficient chemotherapy in mice⁵. Thus, the induction of differentiation of BTICs has been proposed as an approach to target malignant gliomas^{6,7}.

Surrounding glioma cells *in situ* are monocytoïd cells, also referred to as mononuclear phagocytes, which are innate immune cells intrinsic to the CNS (microglia), or those that have infiltrated as circulating monocytes into the compromised CNS to become macrophages. Glioma-infiltrating macrophages and microglia make up a substantial portion of the tumor mass, with some estimates being as high as one in every third cells⁸.

There has been a substantial amount of research into the interactions of macrophages and microglia with gliomas, and whether these cells function to suppress or enhance glioma growth is debated.

Predominantly, gliomas appear to suppress the immune surveillance functions of macrophages and microglia^{9,10} and to respond to their products by increased growth^{11,12} or invasiveness¹³. In contrast, there is evidence that macrophages and microglia attempt to counteract the activity of gliomas. Macrophage and microglia factors stimulate the apoptosis of glioma cells in culture^{14,15} and *in vivo*¹⁶; the toll-like receptor 3 agonist poly(I:C) causes microglia to secrete factors that kill glioma cells in culture¹⁷. Moreover, the stimulation of macrophages and microglia by intratumoral injection of lipopolysaccharide reduces glioma growth in mice¹⁸, whereas the genetic ablation of monocytoïd cells promotes glioma growth¹⁹. Reports are also emerging of the interactions between BTICs and macrophages and microglia. BTICs were found to cause macrophages and microglia to be immunosuppressive²⁰, and macrophages and microglia enhanced the invasiveness of BTICs²¹. These results emphasize that there are multi-dimensional interactions between gliomas and monocytoïd cells, although, in most cases, the macrophage and microglia activity is co-opted by gliomas. Medications that activate macrophages and microglia and cause BTIC differentiation, particularly if these medications are already in human use for other purposes, may be useful to sway the balance toward curbing tumor growth and clinical benefit. Here, we describe an approach to recruit monocytoïd cells to overcome BTICs.

RESULTS

Monocytoïd cells curb BTIC growth *in vitro*
BTICs were isolated from patients with malignant gliomas² and they grew as progressively larger spheres in suspension cultures

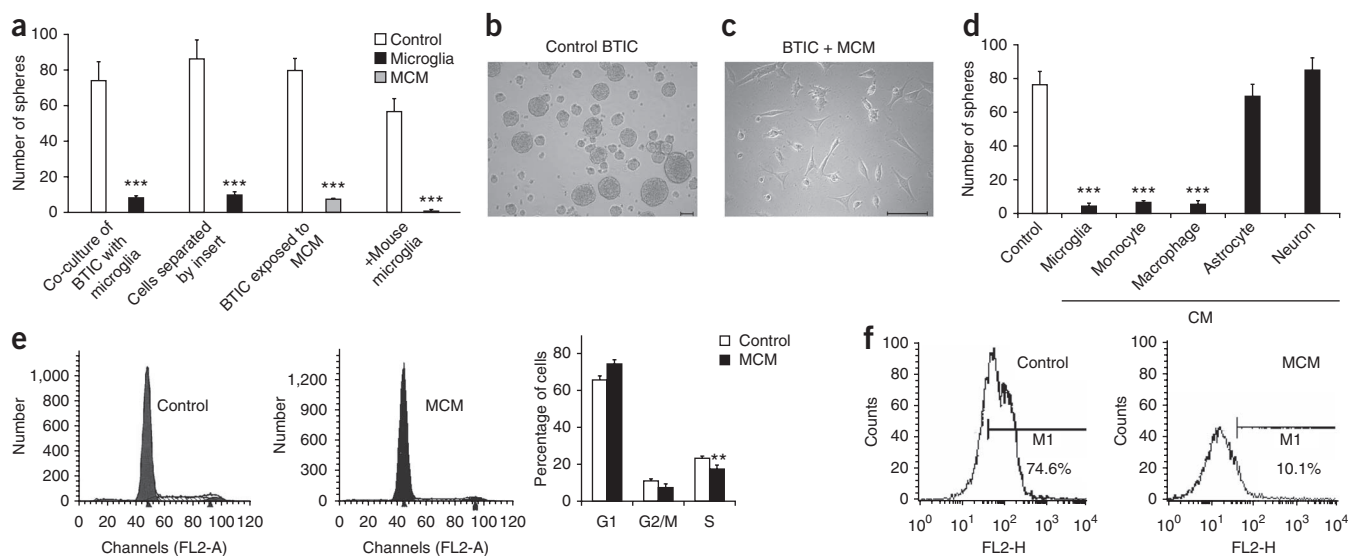


Figure 1: Microglia reduce BTIC spheres in culture. (a) Co-culture of 25EF human BTICs with microglia in cell-cell contact ($P = 1.9 \times 10^{-5}$ with unpaired t test relative to respective control), separated by an insert ($P = 8.0 \times 10^{-6}$ with unpaired t test), using MCM ($P = 6.5 \times 10^{-7}$ with unpaired t test), or co-culture with mouse microglia ($P = 5.0 \times 10^{-6}$ with unpaired t test) decreased the number of BTIC spheres after 72 h ($n = 4$ for all groups). (b,c) Control 25EF BTICs readily formed spheres over 72 h (b), but those exposed to MCM did not (c); instead, cells adhered and differentiated morphologically. Scale bars represent 60 μm . (d) Conditioned medium (CM) from human monocytes or macrophages, but not from astrocytes or neurons, reduced BTIC sphere formation ($P = 4.2 \times 10^{-12}$, $P = 6.5 \times 10^{-12}$, $P = 5.3 \times 10^{-12}$, with ANOVA comparison to control; $n = 4$ for all groups). (e,f) The sphere-reducing property of microglia was corresponded with cell cycle arrest ($P = 3.3 \times 10^{-3}$ with unpaired t test, $n = 4$; e) and decreased CD133 expression (f) of BTICs. Error bars represent s.d. ** $P < 10^{-3}$, *** $P < 10^{-4}$.

that required periodic mechanical dissociation into single cells to maintain them. In serum-free culture medium supplemented with EGF and FGF-2 (referred to here as BTIC medium)², BTIC spheres had stem-like properties, as evidenced by elevated levels of nestin, Sox2, Musashi-1, CD133 and inhibitor of differentiation (ID4) (Supplementary Fig. 1a). When implanted into the brains of NOD-SCID mice, the patient-derived BTICs formed tumors and retained their stem-like markers (Supplementary Fig. 1b).

Non-transformed microglia (Supplementary Fig. 2a) were isolated from surgical resection to treat epilepsy; we previously found that these cells are not activated in non-growth factor supplemented medium by virtue of negligible or low levels of cytokine production^{22,23}. Here, we switched microglia to BTIC medium before experiments to maintain uniform conditions in subsequent co-culture with BTICs. In the BTIC medium, microglia conditioned medium (MCM) collected after 24 h had elevated levels of several cytokines and chemokines (Supplementary Fig. 3), indicating that these cells had become activated. Using 60 μm as the cutoff for sphere size, we found that the co-culture of 10^4 microglia with between 10^3 and 5×10^4 freshly dissociated BTICs in 96-well plates promptly reduced sphere formation (Supplementary Fig. 2b) and corresponded with BTICs adhering to the tissue culture surface. Indeed, co-culture of freshly dissociated BTICs with microglia for 72 h reduced the number of BTIC spheres by over 90% in the 25EF cell line (Fig. 1a) and in the glioma patient-derived BTIC lines 48EF, 69EF and 53M (Supplementary Fig. 2c-e). Notably, the BTIC lines that we used harbor divergent genetic mutations (Supplementary Table 1), but were similarly reduced in sphere-forming capacity by microglia.

All (>30 tested) epilepsy surgery-derived human microglia preparations reduced sphere formation by BTICs. Moreover, the microglia effect involved secreted products, as it was still evident when BTICs and microglia were separated by a culture insert (Fig. 1a) or

when BTICs were exposed to MCM (Fig. 1a-c). MCM was effective at reducing sphere-forming capacity even when diluted 5–10 times before exposure to BTICs (Supplementary Fig. 2f).

To determine whether microglia could affect established spheres, we allowed BTIC lines to grow for 7 d following dissociation. Within hours of exposure of these prominent spheres to MCM, cells began to detach from spheres and to attach onto the tissue culture surface (Supplementary Fig. 2g,h).

We reproduced the effect of human microglia in differentiating human BTICs using conditioned media from mouse microglia (Fig. 1a) and from monocytes and macrophages cultured from peripheral human blood, but not with medium conditioned by human astrocytes or neurons (Fig. 1d). The effect of MCM on BTIC sphere reduction was associated with a reduction of proliferation (Fig. 1e and Supplementary Fig. 2i,j) rather than apoptosis. Finally, the reduced stem-like characteristics of BTICs exposed to MCM was corroborated by the decrease of cells that expressed CD133, a marker of stem-like properties²⁴ (Fig. 1f).

Using an extreme limiting dilution assay²⁵ (Supplementary Fig. 4), we found that spheres developed over 14 d in wells initially plated with 1–200 BTICs; in contrast, no spheres were found in wells plated with similar BTIC numbers when exposed to MCM or MonoCM. Finally, we determined whether there was a divergent effect of monocytoid cells on BTICs versus their more differentiated counterparts. BTICs differentiate in response to 1% fetal bovine serum (FBS)^{2,26} and we noted that, although BTIC growth was readily reduced by co-culture with microglia or by the conditioned media of microglia or monocytes (Supplementary Figs. 5 and 6a,b), these had no obvious effect on the growth of cells differentiated by 1%FBS or on the differentiated U251 or U87 long-term proliferating lines (Supplementary Fig. 6c). Thus, the effect of monocytoid cells was selective for the stem cell compartment.

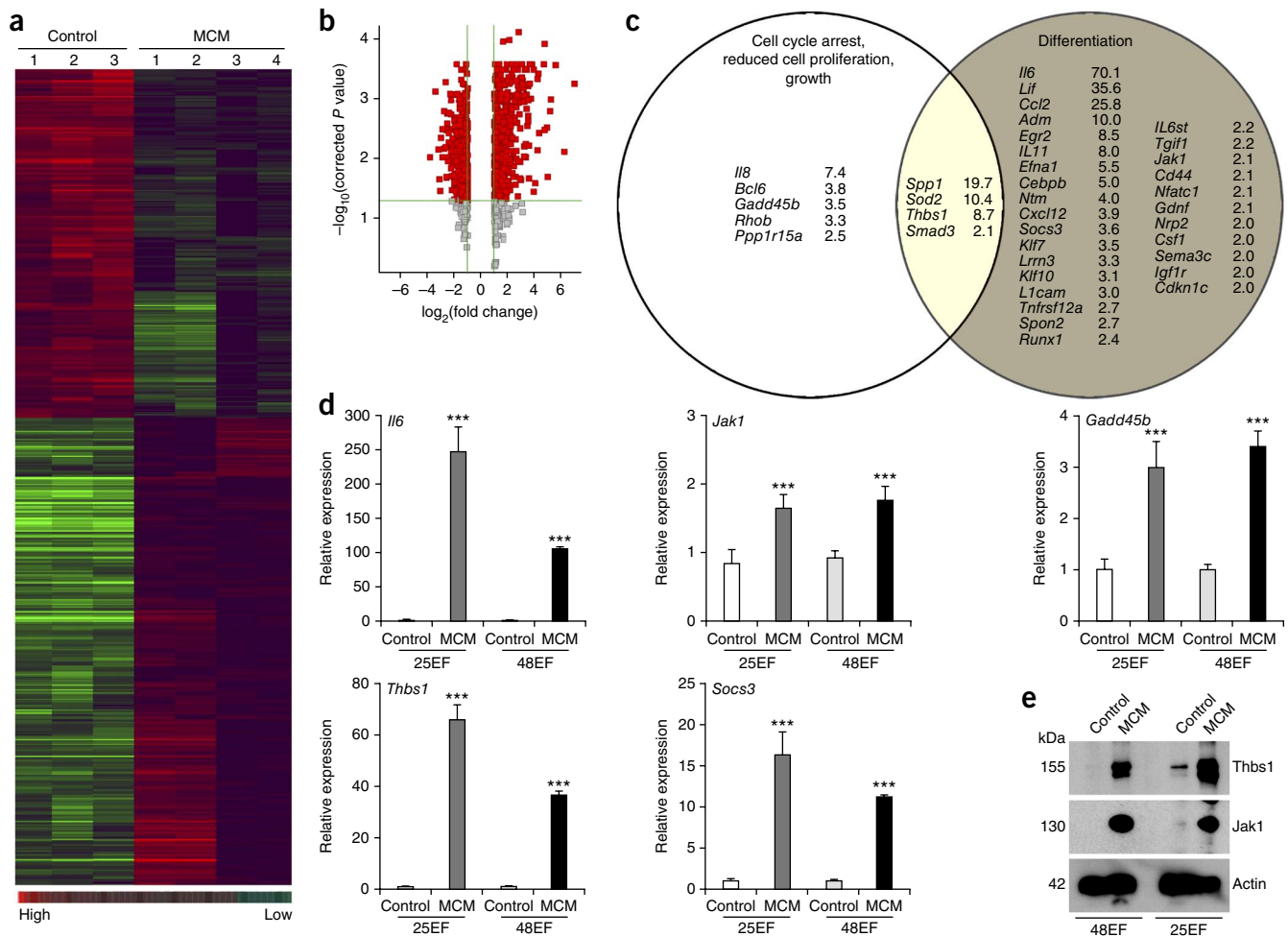


Figure 2: Differential expression of genes in BTICs exposed for 6 h to MCM. (a,b) Hierarchical clustering (a) and volcano plot (b) of differentially expressed genes (GEO accession number [GSE52127](#)) between 25EF controls ($n = 3$) and MCM-exposed ($n = 4$) samples. (c) Several genes involved in cell cycle arrest and reduced cell proliferation and growth or differentiation were significantly upregulated (numbers indicate fold change) by MCM. (d) PCR validation of selected genes in another set of 25EF and 48EF cells with *Gadph* normalization (25EF, $n = 4$ control, $n = 4$ MCM; 48EF, $n = 4$ control, $n = 3$ MCM; for all genes except *Jak1*, where all groups were $n = 3$). $P = 1.0 \times 10^{-5}$ and $P = 7.5 \times 10^{-9}$ with unpaired t test for *Il-6*; $P = 5.0 \times 10^{-3}$ and $P = 6.0 \times 10^{-4}$ with unpaired t test for *Jak1*; $P = 3.1 \times 10^{-4}$ and $P = 8.0 \times 10^{-6}$ with unpaired t test for *Gadd45b*; $P = 5.4 \times 10^{-7}$ and $P = 8.9 \times 10^{-8}$ with unpaired t test for *Thbs1*; $P = 3.2 \times 10^{-5}$ and $P = 1.9 \times 10^{-8}$ with unpaired t test for *Socs3*. (e) *Thbs1* and *Jak1* protein expression following MCM exposure for 6 h and detected via western blots corroborated the rise in transcripts detected for these molecules; full-length gels are shown in Supplementary Figure 10. The elevation in protein levels for IL-6, IL-8 and MCP-1 was corroborated by multiplex analyses (Supplementary Fig. 3). Error bars represent s.d. *** $P < 0.01$.

Mechanisms for reduced BTIC growth

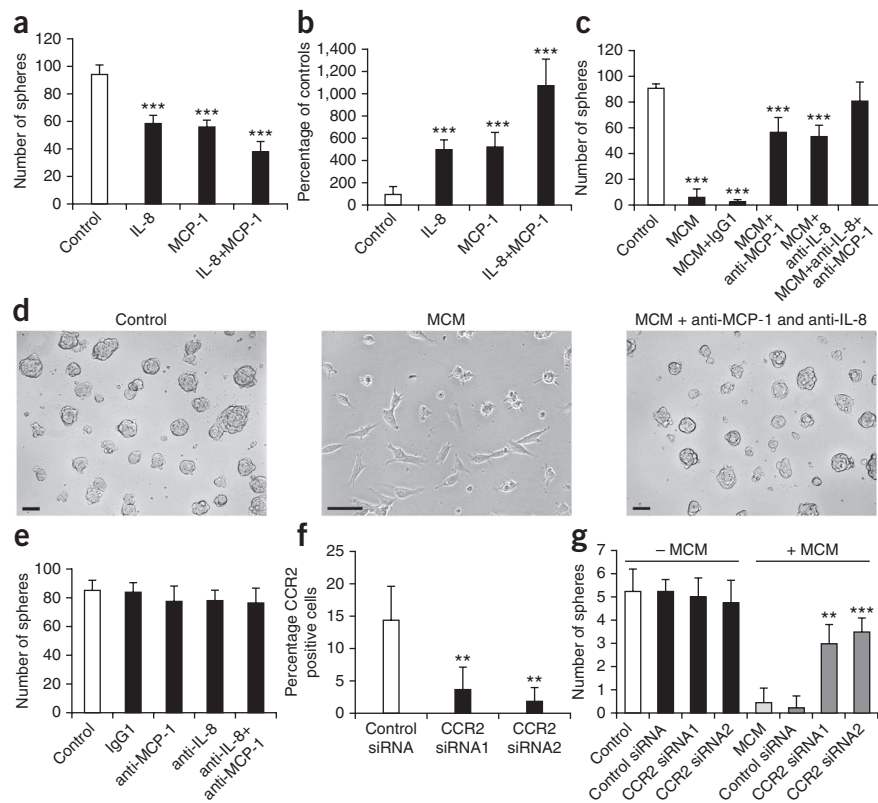
To address the mechanisms by which microglia reduce BTIC growth and promote differentiation, we subjected BTICs to microarray analyses for 39,000 genes. We identified 1,098 ($P < 0.05$) genes in BTICs that were differentially expressed at 6 h with MCM treatment compared with controls (Fig. 2a,b). As some genes were represented by more than one probe on the chip, we also generated probe-set averages using GeneSpring's gene level expression function (GEO accession number [GSE52127](#)).

As seen by functional annotation clustering, a large number of transcripts of genes involved in decreasing cellular growth and/or increasing differentiation were upregulated by MCM (Fig. 2c,d); western blots (Fig. 2e) and ELISAs (interleukin (IL)-6, IL-8 (CXCL8) and macrophage chemoattractant protein-1 (MCP-1, CCL2); Supplementary Fig. 3) corroborated the upregulation of these genes at the level of protein expression. Conversely, transcripts for the stem-like markers

Sox2 and ID4 were reduced in BTICs by MCM (3.9- and 4.5-fold, respectively); transcripts for nestin, Musashi-1 and CD133 were too close to the detection limit for reliable quantitation.

Next, we sought to address the mechanisms by which microglial factors curb BTICs. We examined MCM using multiplex protein analyses (luminex^R) and found that MCP-1, IL-8 and several other factors (Supplementary Fig. 3) were present at high concentrations in MCM. We focused on MCP-1 and IL-8 as potential factors that reduce BTIC growth, as MCP-1 differentiates neuroprogenitor cells and astrocytes²⁷ and IL-8 promotes neural cell differentiation²⁸. First, we addressed whether the application of recombinant human chemo-kines could reduce sphere formation by freshly dissociated BTICs. Either IL-8 or MCP-1 alone decreased BTIC sphere formation, and they had a more robust effect when used in combination (Fig. 3a); these outcomes were paralleled by an increase in the number of cells that adhered and morphologically differentiated (Fig. 3b),

Figure 3: Microglia-derived factors involved in BTIC growth reduction. (a,b) IL-8 and MCP-1 expression reduced the number of 25EF BTIC spheres at 72 h (IL-8, $P = 2.0 \times 10^{-5}$; MCP-1, $P = 1.0 \times 10^{-5}$; IL-8 + MCP-1, $P = 1.5 \times 10^{-7}$; ANOVA comparison with control, $n = 4$ for all groups; a) and increased the percentage of the cells that were differentiated (IL-8, $P = 7.0 \times 10^{-9}$; MCP-1, $P = 5.9 \times 10^{-9}$; IL-8 + MCP-1, $P = 1.5 \times 10^{-12}$; ANOVA comparison with control, $n = 4$ for all groups; b). (c,d) The MCM-induced reduction of BTIC spheres was overcome by function-blocking antibodies to MCP-1 and/or IL-8 (MCM, $P = 9.2 \times 10^{-10}$; MCM + IgG1, $P = 5 \times 10^{-10}$; MCM + MCP-1 antibody, $P = 5.0 \times 10^{-4}$; MCM + IL-8 antibody, $P = 1.3 \times 10^{-4}$; ANOVA comparison with control, $n = 4$ for all groups). Scale bars represent 100 μm . (e) These function-blocking antibodies had no direct effect on BTICs ($P = 0.684$, $n = 4$ all groups). (f,g) Two siRNAs reduced CCR expression in BTICs (siRNA1, $P = 8.2 \times 10^{-3}$; siRNA2, $P = 3.1 \times 10^{-3}$; ANOVA compared with control siRNA, $n = 4$ for all groups; f) and increased their resistance to MCM (siRNA1, $P = 1.5 \times 10^{-3}$; siRNA2, $P = 1.4 \times 10^{-4}$; ANOVA comparison with MCM, $n = 4$ for all groups; g). These results were reproduced in 48EF and 53M lines. Error bars represent s.d. ** $P < 0.01$, *** $P < 0.001$.



consistent with decreased cell cycle progression, as observed with propidium iodide flow cytometry (IL-8 + MCP-1 = $17.8 \pm 2.1\%$, control = $24.3 \pm 0.8\%$, $n = 3$ control, and $n = 3$ IL-8 + MCP-1, $P = 0.007$). In addition, the marked reduction of BTIC spheres in response to MCM was neutralized by the addition of function blocking antibodies to IL-8 and MCP-1 (Fig. 3c,d). Notably, the antibodies had no effect on control BTIC cells either alone or in combination (Fig. 3e). Finally, we lowered the expression of CCR2, the receptor for MCP-1, in BTICs using RNAi (Fig. 3f) and found that the cells became less responsive to the reduction of BTIC spheres elicited by MCM (Fig. 3g). Together, these results suggest that the IL-8 and MCP-1 produced by microglia contribute to the reduced proliferation and increased differentiation of BTICs. It is likely that other cytokine and non-cytokine molecules produced by microglia contribute to the growth-reducing property on BTICs. For instance, we found that TNF- α , which was elevated in MCM (Supplementary Fig. 3), also reduced BTIC sphere formation (30% reduction at 20 ng ml $^{-1}$ TNF- α).

AmpB-activated microglia curb BTIC growth further

We tested a collection of 1,040 compounds (NINDS Custom Collection II, MicroSource Discovery) for their capacity to further activate human microglia that have been stimulated with the toll-like receptor (TLR) agonist lipopolysaccharide (LPS). Using the increase in TNF- α level in cell culture medium as the screen, we identified Amphotericin B (AmpB) as a hit (Fig. 4a). The complete analysis of the drug screen is reported elsewhere²⁹. Subsequent analyses revealed that AmpB increased TNF- α expression in microglia (Fig. 4b) and macrophages (data not shown) without the necessity of LPS priming; AmpB did not stimulate BTICs directly. AmpB stimulation of wild-type macrophages to produce TNF- α was reduced by 60% in macrophages from TLR-2 null mice and by >95% in macrophages from MyD88 and TRIF double knockout mice (data not shown); a deficiency of these two pathway adaptors abrogates signaling from

all TLRs. These results implicate TLR signaling in the mechanism by which AmpB stimulates monocytoid cells.

Next, we examined the effect of AmpB-stimulated microglia and found that they further increased the microglia-induced differentiation of BTICs. This was less apparent when the number of spheres was documented at 72 h, as the control MCM had already reduced sphere formation by over 95%, but when the number of cells that had attached onto the substratum at 6 h was evaluated for whether they had morphologically differentiated (that is, adhered cells that have expanded in dimensions from a rounded to a flattened morphology that includes processes), the additional activity of AmpB exposed microglia, over that of microglia alone, was evident for both the 25EF (Fig. 4c,d) and 48EF (data not shown) lines. Notably, we discovered that AmpB added alone to BTICs did not alter sphere formation, highlighting the necessity for the intermediary of microglia. That AmpB was without direct activity on BTICs was supported by the results that AmpB did not increase the minimal levels of cytokines and chemokines that BTICs produce (Supplementary Fig. 3).

We analyzed the nature of the BTIC cells that adhered in response to MCM alone or to AmpB and MCM. BTIC spheres contained cells that expressed GFAP, β III tubulin, nestin and Sox2, markers of astrocytes, neurons and early precursors, respectively. Following 6 h of treatment, there were more astrocytes and neurons in cultures treated with AmpB and MCM than in those treated with MCM alone, whereas nestin and Sox2 were correspondingly reduced (Fig. 4e,f); these results were corroborated by western blot analyses (Fig. 4g). Thus, microglia promote the differentiation of BTICs into astrocytes and neurons, and further stimulation of microglia with AmpB enhanced this response.

AmpB reduces BTIC tumorigenicity in mice

BTICs are highly tumorigenic in nature, and as few as 100 25EF cells were sufficient to produce intracranial grafts that killed mice; a dose-related

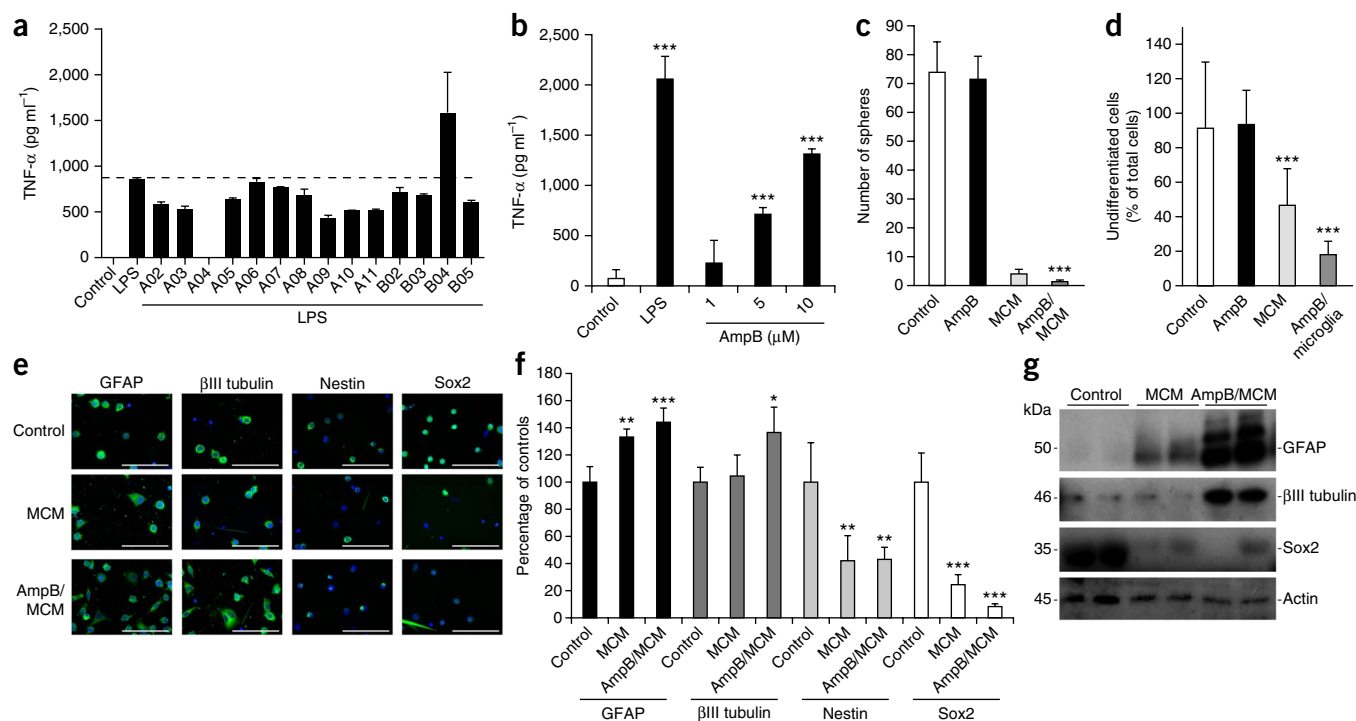


Figure 4: AmpB promotes the microglial differentiation of BTICs. (a) Example of a screen showing further elevation of TNF- α in LPS-stimulated microglia; AmpB is #B04 and 1,040 medications were screened²⁹. (b) AmpB alone stimulated microglia (LPS, $P = 1.3 \times 10^{-12}$; 5 μ M AmpB, $P = 3.1 \times 10^{-7}$; 10 μ M AmpB, $P = 3.0 \times 10^{-11}$; ANOVA comparison with control, $n = 4$ for all groups). (c,d) AmpB itself did not affect BTICs, but its stimulation acted to, via microglia, reduce spheres ($P = 1.8 \times 10^{-8}$ with ANOVA comparison with control, $n = 4$ for all groups; c) and to promote morphological differentiation of adhered 25EF cells (MCM, $P = 5.6 \times 10^{-10}$; MCM + AmpB, $P = 2.7 \times 10^{-12}$; ANOVA comparison with control, $n = 4$ for all groups; d). (e,f) Immunofluorescence images (e) and quantitation (f) of adhered cells after 6 h revealed that AmpB promoted the microglial differentiation of BTICs into astrocytes and neurons while reducing the expression of the stem-like markers nestin and Sox2 (left to right, ANOVA comparison to respective control, and $n = 4$ for all groups: GFAP: MCM, $P = 2.2 \times 10^{-3}$; AmpB + MCM, $P = 3.0 \times 10^{-4}$; β III tubulin: AmpB + MCM, $P = 0.02$; nestin: MCM, $P = 0.008$; AmpB + MCM, $P = 0.009$ for nestin; Sox2: MCM, $P = 5.3 \times 10^{-5}$; AmpB + MCM, $P = 1.1 \times 10^{-5}$). Scale bars represent 100 μ m. (g) These results were corroborated by western blots; full-length gel is shown in Supplementary Figure 10. Error bars represent s.d. * $P = 0.02$, ** $P < 0.01$, *** $P < 0.001$.

effect was documented with higher numbers of implants proportionally reducing survival (Supplementary Fig. 7a). We implanted the 25EF and 48EF human BTIC lines into the right striatum of NOD-SCID mice and initiated daily treatment with AmpB (0.2 mg per kg of body weight per d, intraperitoneal) or vehicle 7 d after. The therapeutic efficacy of AmpB was first determined 7 weeks post implantation in live asymptomatic mice using T2-weighted magnetic resonance imaging (MRI). MRI images revealed a marked reduction of tumor mass in AmpB-treated mice when compared with vehicle-injected controls (Fig. 5a,b and Supplementary Fig. 7b,c).

We killed a group of asymptomatic 25EF-implanted mice at 7 weeks post-implantation and evaluated hematoxylin- and eosin-stained sections. Tumor mass in vehicle-treated control mice was noticeably larger than that in AmpB-treated mice (Fig. 5c). Moreover, the tumors in control mice showed a higher proliferation index, as evidenced by Ki67 staining, whereas those treated with AmpB had markedly lower Ki67 labeling (Fig. 5d); the latter was still higher than that of the negative host brain, as AmpB reduced tumor growth, but did not prevent tumor formation altogether. Notably, Iba1 staining for macrophages and microglia was elevated in the AmpB or LPS (used as another activator control, albeit of less potential utility than AmpB clinically) treatment groups compared with the vehicle-treated controls (Fig. 5e). The massive activation of macrophages and microglia, particularly toward a pro-inflammatory, tumor-resisting phenotype (M1)³⁰, was corroborated by increased representation of iNOS-expressing M1 cells in AmpB-treated mice (Fig. 5e). Finally, tumor volume was significantly reduced in AmpB-treated mice compared

with vehicle controls (AmpB, 300 ± 120 mm³; vehicle, 750 ± 60 mm³; $n = 4$ each, $P = 0.0005$).

Mice with intracerebral gliomas gradually lose weight and eventually die from the expanding tumor mass. We followed NOD-SCID mice implanted intracranially with BTICs and treated with daily AmpB (0.2 mg per kg, intraperitoneal) from a week after implantation. We found that AmpB treatment prevented weight loss (Supplementary Fig. 7d) and prolonged survival. In mice with implanted 25EF cells, all of the control mice died within 80 d, but AmpB treatment prolonged survival to 130 d (Fig. 5f). In mice implanted with 48EF cells, daily treatment with vehicle from 7 d post-implantation resulted in all of the mice dying by 70 d, but AmpB treatment more than doubled their survival time (Fig. 5g).

Safety of low dose AmpB in mice

When given at high doses, AmpB toxicity includes nephrotoxicity, leukopenia and other complications. Serum concentrations attained in humans given these high doses of AmpB ranged from 500 to 2,000 ng ml⁻¹ (<http://www.drugs.com/>). Thus, we addressed the safety of AmpB at 0.2 mg per kg by harvesting normal NOD-SCID mice 30 d after daily intraperitoneal injections. A mean serum level of 56 ng ml⁻¹ AmpB, which is at least tenfold less than that found in humans, was seen 2 h after the last of 30 injections (Supplementary Fig. 8a). Moreover, analysis of the brain tissue from AmpB-treated tumor bearing mice revealed elevated levels of AmpB in the brain compared with those in control mice, suggesting that AmpB indeed reached the brains

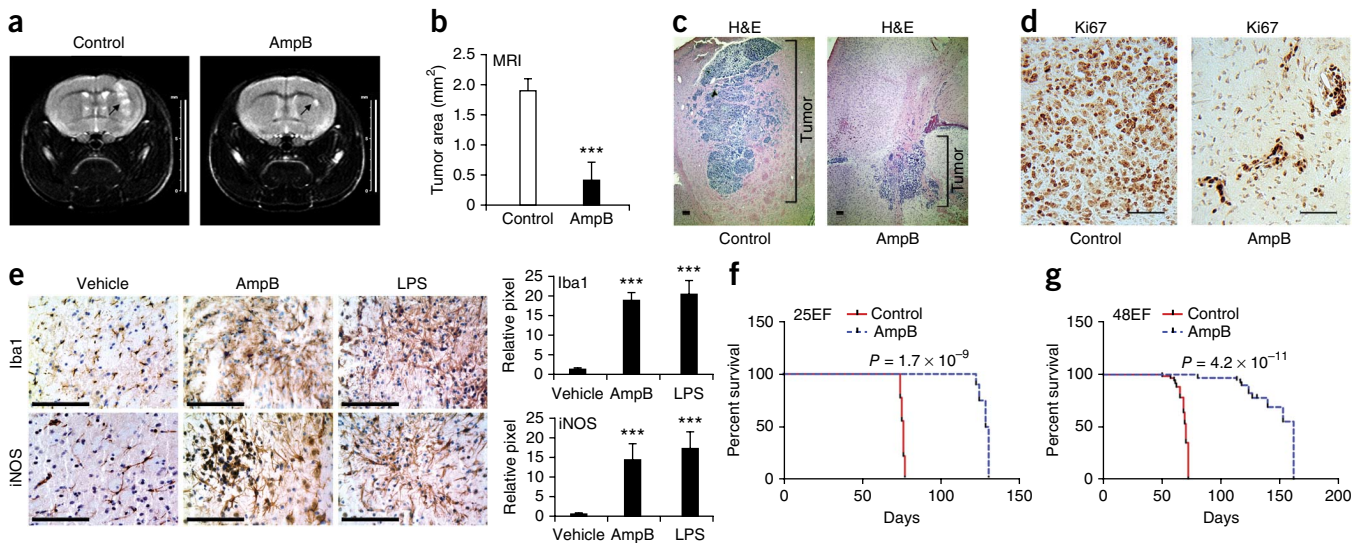


Figure 5: AmpB reduces intracranial growth of patient-derived BTICs in mice. (a–d) MRI at 7 weeks post-implantation of 25EF BTICs revealed that the large tumor mass (arrow) in control mice was reduced by AmpB treatment ($n = 4$ each; $P = 3.1 \times 10^{-4}$ with unpaired t test; a,b), and this was validated by hematoxylin and eosin (H&E, c) and Ki67 (d) staining. Scale bars represent 100 μm . (e) AmpB treatment increased immunoreactivity for Iba1 and iNOS in and around the implanted tumor to the same extent as LPS, and decreased tumor volume (Iba1: AmpB, $P = 5.1 \times 10^{-9}$; LPS, 5.1×10^{-9} ; ANOVA comparison with vehicle, $n = 4$ for all groups; iNOS: AmpB, $P = 8.5 \times 10^{-7}$; LPS, $P = 9.9 \times 10^{-8}$; ANOVA comparison with vehicle, $n = 4$, $n = 5$ AmpB and $n = 6$ LPS). (f,g) At 7 weeks, Kaplan-Meier analysis revealed that AmpB extended the lifespan of mice implanted with 25EF ($n = 8$ vehicle, $n = 8$ AmpB; f) or 48EF ($n = 12$ vehicle, $n = 12$ AmpB, log-rank analysis; g). Error bars represent s.d. *** $P < 0.001$.

of mice with prolonged treatment with or without compromising the blood-brain barrier (Supplementary Fig. 8b).

When blood was taken for differential cell counts, there was no loss of neutrophils, whereas monocyte levels were increased in

AmpB-treated non-tumor implanted mice (Supplementary Fig. 8c). A similar lack of neutropenia and increased monocytes counts were found in 25EF-implanted mice treated daily with AmpB (0.2 mg per kg) for 50 d, and their urine specimens registered normal results (Supplementary Fig. 8d,e). Thus, a low dose of AmpB can be used chronically to curb tumor growth without substantial toxicity.

AmpB requires monocytoid cells to curb BTICs

We addressed the necessity of macrophages and microglia in the mechanism by which AmpB reduced tumor growth in mice. First, we evaluated *ex vivo* exposed BTICs for their subsequent intracranial growth in mice. MRI images taken 70 d after implantation of control 48EF cells showed a huge tumor mass in mice, and this was equally large in mice implanted with BTICs that were exposed *ex vivo* to AmpB without microglia intermediary. In contrast, a trend toward

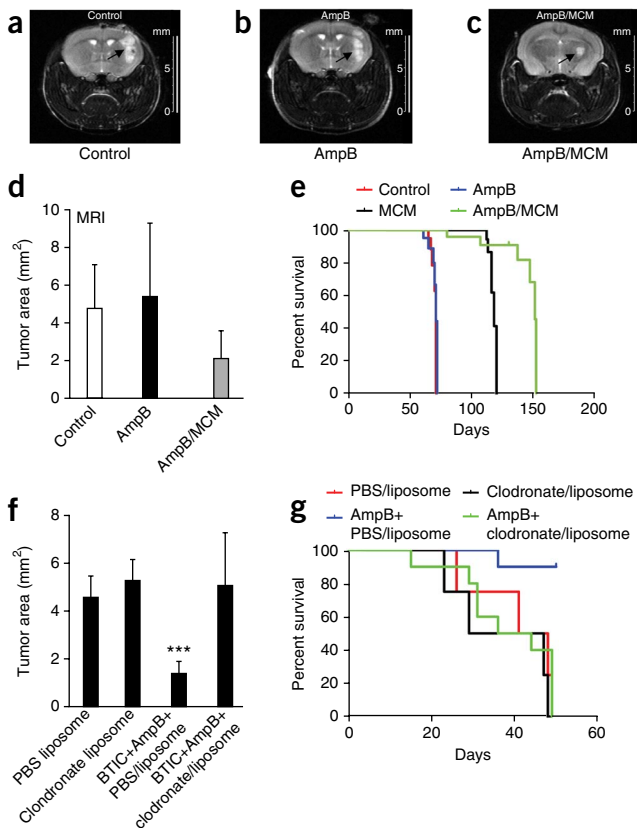


Figure 6: The AmpB amelioration of BTIC intracranial growth requires monocytoid cells. (a–e) BTICs (48EF) exposed *ex vivo* to AmpB grew similarly to control BTICs in mice, unless they were pre-exposed to AmpB-stimulated microglia (AmpB/MCM); this is suggested by an MRI trend in symptomatic mice at 70 d ($P = 0.2$ with ANOVA comparison of AmpB/MCM to control; control, $n = 3$; AmpB, $n = 4$; AmpB + MCM, $n = 4$; a–d) and survival ($n = 6$ for all groups, $P = 0.0129$ comparing AmpB/MCM to MCM, $P = 6.7 \times 10^{-4}$ comparing AmpB/MCM to control, using log-rank analysis; e). (f) AmpB (and PBS liposome) injected daily from 7 d post-implant ameliorated tumor size (7 weeks MRI; $n = 3$ BTIC + PBS/liposome, $n = 3$ BTIC + clodronate/liposome, $n = 5$ BTIC + AmpB + PBS/liposome, $n = 5$ BTIC + AmpB + clodronate/liposome; *** $P = 0.003$ with ANOVA comparison between AmpB + PBS/liposome and AmpB + clodronate/liposome groups). (g) AmpB treatment of mice with intracranial BTICs extended survival when control PBS/liposome mice administered, whereas this benefit was lost in clodronate/liposome mice ($P = 0.0001$ when comparing AmpB + PBS/liposome with all other groups, log-rank analysis, $n = 4$ PBS/liposome, $n = 4$ clodronate/liposome, $n = 10$ AmpB + PBS/liposome, $n = 10$ AmpB/clodronate liposome). Error bars represent s.d.

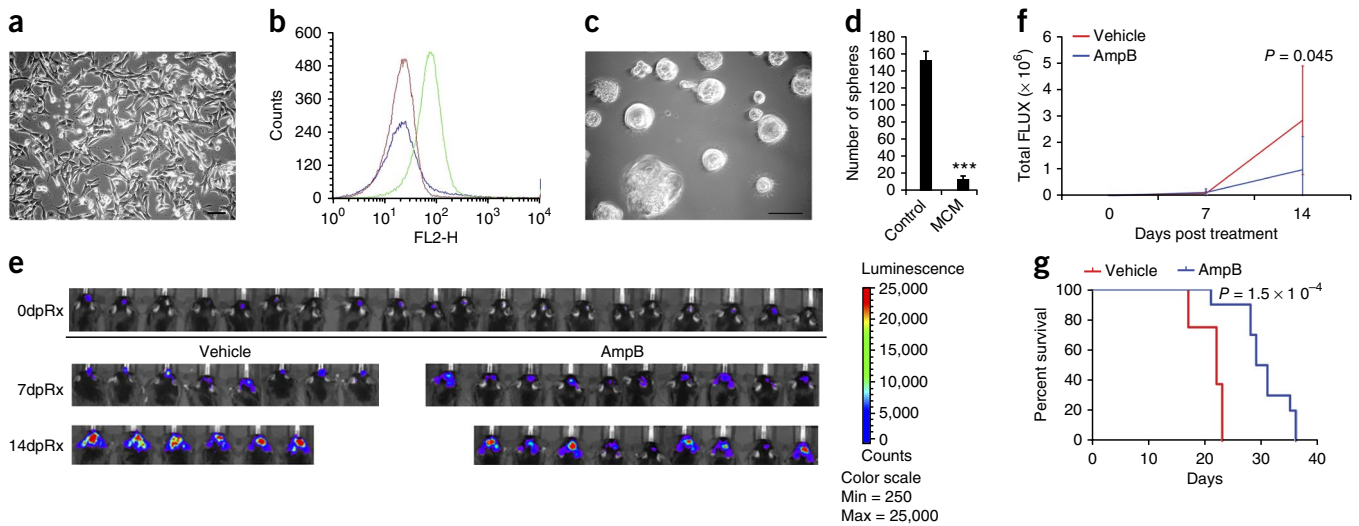


Figure 7: AmpB reduces tumor growth and prolongs the survival of immunocompetent mice with syngeneic BTICs. (a) The C57BL/6 mouse glioma line GL261 grew as adherent cells in serum-containing medium. Scale bar represents 100 μ m. (b) When sorted using antibody-coated magnetic beads, flow cytometry analysis revealed an enrichment from <0.5% of CD133⁺ cells (red line; blue line indicates isotype control) to over 50% (green line). (c,d) CD133⁺-enriched cells grown in serum-free BTIC medium formed floating spheres (c), but this was abrogated when cells were exposed to mouse MCM (d) ($n = 4$, $***P = 3.7 \times 10^{-7}$ with unpaired t test). Scale bar represents 100 μ m. (e,f) Bioluminescence obtained at day 7 after implantation of CD133⁺ GL261 cells (0dpRx) and at days 7 and 14 after treatment (7dpRx and 14dpRx); the decreasing number of mice ($n = 6$ vehicle, $n = 9$ AmpB at 14 d) at progressive time points is a result of the death of the mice. At death, the brains of mice contained cells that were positive for CD133 and nestin (Supplementary Fig. 8f). (g) Kaplan-Meier analysis revealed that AmpB extended the lifespan of mice implanted with CD133⁺ mouse BTICs ($n = 9$ vehicle, $n = 11$ AmpB). Error bars represent s.d.

a smaller tumor mass was apparent in mice implanted with BTICs that were previously exposed to conditioned medium from AmpB-activated microglia (Fig. 6a–d).

Survival curve analyses revealed that mice in the control group died around day 70, as did mice implanted with BTICs that were exposed *ex vivo* to AmpB without microglia intermediary (AmpB group; Fig. 6e). In contrast, mice implanted with BTICs that were previously exposed to MCM had significantly longer survival periods, and this was exceeded (150 d) in mice harboring BTICs that had been pre-exposed *ex vivo* to AmpB-treated microglia (AmpB/MCM group, $n = 6$ for all groups; $P = 0.0129$ compared with MCM, $P = 6.7 \times 10^{-4}$ compared with the others; Fig. 6e).

We implanted BTICs into NOD-SCID mice and initiated weekly intravenous infusion of liposomes containing clodronate (dichloromethylene bisphosphonate) 7 d later to deplete circulating monocytes³¹ and CNS macrophages³². Daily intraperitoneal AmpB (0.2 mg per kg) or saline treatment was also initiated 7 d post-implant. MRI analyses at 7 weeks revealed that, in mice receiving control (phosphate-buffered saline, PBS) liposomes, AmpB reduced tumor size as anticipated; however, this therapeutic effect was eliminated in mice treated with clodronate liposomes (Fig. 6f). Finally, although mice treated with PBS liposomes and AmpB remained alive, mice treated with clodronate liposomes with reduced monocyte counts in blood (AmpB + clodronate/liposome, $1.5 \pm 1.3\%$ of total cells counted; AmpB + PBS/liposome, $6 \pm 2.3\%$; $n = 4$ each, $P = 0.0145$) and less Iba1⁺ cells in the brain (AmpB + clodronate/liposome, $43,541.7 \pm 12,385.3$ pix-els; AmpB + PBS/liposome, $130,540.7 \pm 53,717.6$ pixels; $n = 3$ each, $P = 0.0099$) were no longer protected by AmpB (Fig. 6g). Together, our results indicate that AmpB requires monocytoïd cells as an inter-mediary to reduce BTIC growth.

Efficacy of AmpB in syngeneic immunocompetent mice

Given that human BTICs were used as the implants described above, the recipient mice were necessarily immune-compromised to prevent

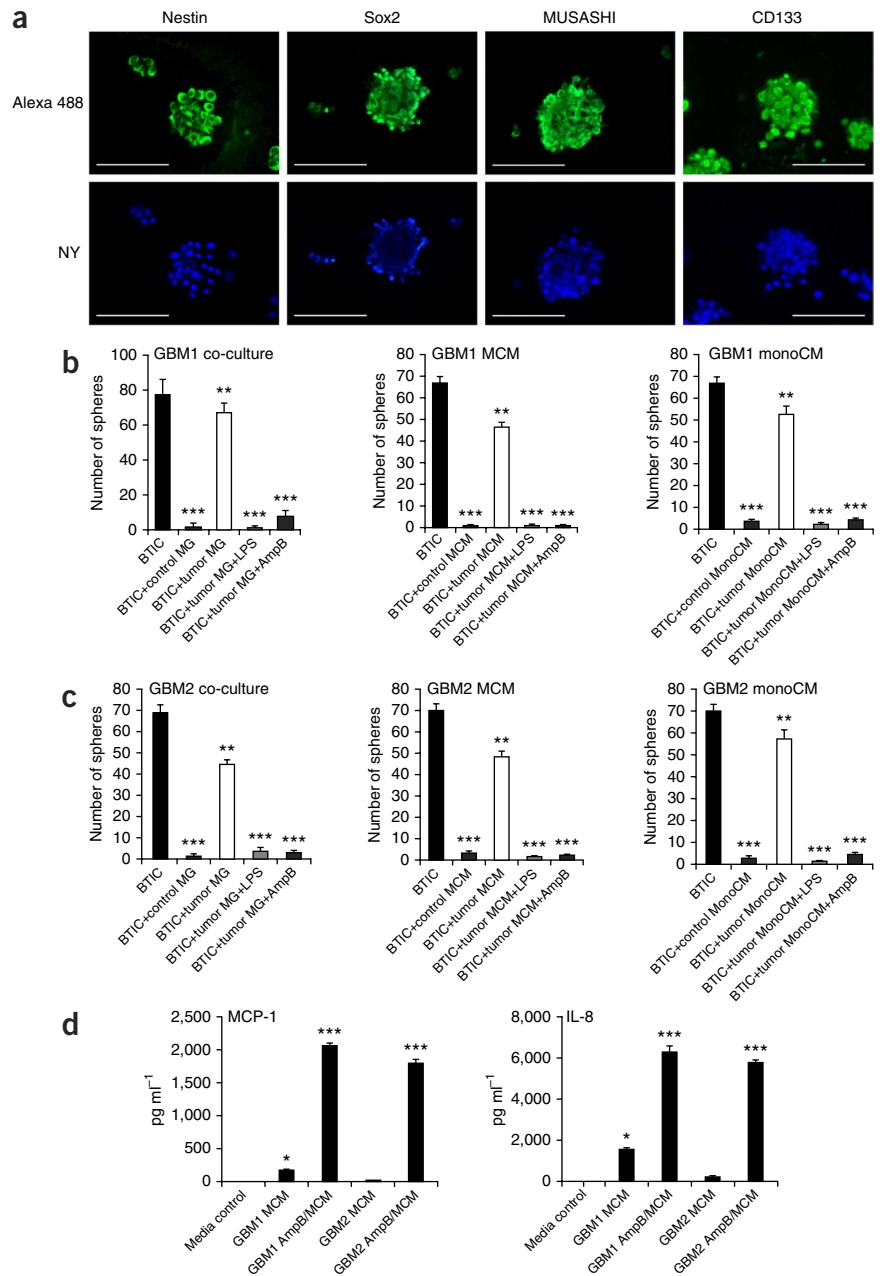
tumor rejection. We therefore extended our studies to mice with normal immunity. We used the GL261 glioma line of C57BL/6 origin³³ (Fig. 7a), previously transfected with a luciferase (LUC) construct, and enriched stem-like CD133⁺ cells from <0.1% to >50% via antibody-coated magnetic bead separation (Fig. 7b). When the CD133⁺ sorted cells were grown in BTIC medium, they formed prominent spheres (Fig. 7c), but this was prevented by exposure to mouse MCM (Fig. 7d).

GL261 CD133⁺ enriched cells were implanted into the right striatum of C57BL/6 mice. We used bioluminescence imaging 7 d later to determine intracerebral tumor size, and mice with comparable tumors were randomly segregated into groups for daily treatment with AmpB (0.2 mg per kg per d, intraperitoneal) or vehicle. Bioluminescence imaging was conducted again 7 and 14 d post treatment in surviving mice (Fig. 7e) and we found a substantial reduction of tumor growth in mice treated with AmpB at the latter treatment period (Fig. 7f). Consistent with this observation, AmpB prolonged the average survival of mice by 44% (Fig. 7g). Thus, the therapeutic efficacy of AmpB was apparent in immunocompetent mice, even against the highly aggressive CD133⁺ G261 tumor.

Stimulation of GBM-derived microglia and monocytes by AmpB

The microglia that we used in our experiments were from surgical resections to treat epilepsy, raising the question of whether microglia from glioma patients would be similarly efficacious. We obtained glioblastoma specimens and blood from six subjects (referred to as GBM1–6) fresh from the operating theater and derived microglia and BTICs. Given that BTICs from three subjects did not grow in culture, cells from four patients were analyzed. Notably, microglia, MCM or MonoCM (conditioned medium from peripheral blood-derived monocytes) from glioblastoma subjects could not reduce autologous (GBM1–4; Fig. 8, Supplementary Fig. 9 and data not shown) or heterologous (25EF and 48EF; Supplementary Fig. 9) BTIC growth under conditions in which control microglia robustly inhibited BTIC

Figure 8: Microglia and monocytes from glioblastoma patients do not curb autologous BTIC growth in culture, but this is rectified by AmpB treatment. (a) BTICs from a glioblastoma resection (GBM1) expressed stem-like markers. NY, nuclear yellow. (b,c) BTICs from GBM1 (b) or GBM2 (c) were not reduced in sphere formation when exposed to co-culture of autologous microglia (MG), MCM or with conditioned medium of autologous blood-derived monocytes (monoCM), but this was normalized by AmpB (or LPS) treatment. Control refers to specimens from a non-glioma subject (GBM1 co-culture; BTIC + control MG, $P = 1.0 \times 10^{-11}$; BTIC + tumor MG + LPS, $P = 9.2 \times 10^{-12}$; BTIC + tumor MG + AmpB, $P = 3.0 \times 10^{-11}$; ANOVA comparison to BTIC alone; BTIC + tumor MG, $P = 3.1 \times 10^{-10}$; comparison of tumor MG to tumor MG + AmpB; $n = 4$ for all groups; GBM1 MCM: BTIC + control MCM, $P = 1.6 \times 10^{-12}$; BTIC + tumor MCM + LPS, $P = 1.6 \times 10^{-12}$; BTIC + tumor MCM + AmpB, $P = 1.6 \times 10^{-12}$; ANOVA comparison to BTIC alone; BTIC + tumor MCM, $P = 9.7 \times 10^{-11}$; comparison of tumor MCM to tumor MCM + AmpB; $n = 4$ for all groups; GBM1 monoCM: BTIC + control MG, $P = 3.8 \times 10^{-11}$; BTIC + tumor MG + LPS, $P = 2.7 \times 10^{-11}$; BTIC + tumor MG + AmpB, $P = 4.2 \times 10^{-11}$; ANOVA comparison to BTIC alone; BTIC + tumor MG, $P = 1.6 \times 10^{-9}$; comparison of tumor monoCM to tumor monoCM + AmpB; $n = 4$ for all groups; GBM2 co-culture; BTIC + control MG, $P = 1.2 \times 10^{-11}$; BTIC + tumor MG + LPS, $P = 1.8 \times 10^{-11}$; BTIC + tumor MG + AmpB, $P = 1.6 \times 10^{-11}$; ANOVA comparison to BTIC alone; BTIC + tumor MG, $P = 1.0 \times 10^{-8}$; comparison of tumor MG to tumor MG + AmpB; $n = 4$ for all groups; GBM2 MCM: BTIC + control MG, $P = 1.8 \times 10^{-12}$; BTIC + tumor MG + LPS, $P = 1.7 \times 10^{-12}$; BTIC + tumor MG + AmpB, $P = 1.8 \times 10^{-12}$; ANOVA comparison to BTIC alone; BTIC + tumor MG, $P = 1.7 \times 10^{-10}$; comparison of tumor MCM to tumor MCM + AmpB; $n = 4$ for all groups; GBM2 monoCM: BTIC + control MG, $P = 3.1 \times 10^{-11}$; BTIC + tumor MG + LPS, $P = 2.3 \times 10^{-11}$; BTIC + tumor MG + AmpB, $P = 4.5 \times 10^{-11}$; ANOVA comparison to BTIC alone; BTIC + tumor MG, $P = 1.0 \times 10^{-9}$; comparison of tumor monoCM to tumor monoCM + AmpB; $n = 4$ for all groups). (d) Microglia from GBM1 or GBM2 produced minimal MCP-1 or IL-8 until exposed to AmpB (MCP-1: GBM1 MCM, $P = 0.006$ versus media control; GBM1 AmpB/MCM, $P = 1.3 \times 10^{-12}$ versus GBM1 MCM; GBM2 AmpB/MCM, $P = 1.3 \times 10^{-12}$ versus GBM2 MCM; ANOVA, $n = 4$ for all groups; IL-8: GBM1 MCM, $P = 4.0 \times 10^{-6}$ versus media control; GBM1 AmpB/MCM, $P = 2.0 \times 10^{-12}$ versus GBM1 MCM; GBM2 AmpB/MCM, $P = 1.3 \times 10^{-12}$ versus GBM2 MCM; ANOVA, $n = 4$ for all groups). Error bars represent s.d. * $P < 0.001$, ** $P < 10^{-7}$, *** $P < 10^{-10}$.



sphere formation. Treatment of GBM-derived microglia or monocytes with AmpB or LPS in culture re-enabled their capacity to reduce autologous BTIC sphere formation.

Our results (Fig. 3) implicate MCP-1 and IL-8 in the microglia reduction of BTIC growth. Thus, we addressed whether microglia from the GBM subjects lacked these molecules and, indeed, we found low levels of expression (Fig. 8d). Following activation with AmpB, marked elevation of MCP-1 (to equivalent levels in non-glioma microglia; Fig. 8 and Supplementary Fig. 3) and IL-8 (to ~30% of non-glioma microglia; and Fig. 8 and Supplementary Fig. 3) occurred. Overall, these results indicate that monocytoid cells are compromised

in glioma patients and that the activation of these cells with AmpB re-enables their capacity to curb BTIC growth.

DISCUSSION

The conversion of BTICs into more differentiated progenies that are amenable to chemotherapies has been proposed as a means to treat glioblastomas^{6,7,34}. We found that non-glioma-associated monocytoid cells differentiate BTICs, whereby the latter decrease their proliferation rate, reduce their stem-like markers, and acquire proteins of the astrocyte and neuronal lineages. Cellular differentiation was also consistent with adhesion of cells that had detached from floating

spheres and the morphological differentiation of adhered cells. The mechanism accounting for cellular differentiation is consistent with the upregulation of genes known to promote cell cycle arrest and increased differentiation (Fig. 2). We note that, although the reduction of proliferation and differentiation of BTICs is a major outcome of the monocytoid response, there could also have been alteration of asymmetric versus symmetric division, cell-cell or cell-substrate adhesion parameters, or the differentiation of BTICs to a cell type that does not form spheres. Of importance, the effect of monocytoid cells on reducing growth was found to be BTIC-specific, and was not obvious in cells differentiated from BTICs by FBS, or in the differentiated glioma lines U87 and U251.

We found that the monocytoid-induced differentiation of BTICs was promoted by AmpB treatment and that AmpB treatment of mice with xenogeneic or syngeneic BTICs extended lifespan substantially. Moreover, we noted that monocytes and microglia from glioblastoma patients were unable to reduce BTIC sphere formation until they received AmpB. To the best of our knowledge, this is the first report of a US Food and Drug Administration-approved medication that has the capacity to reduce the proliferation of BTICs and induce their differentiation.

Although our initial focus was CNS-intrinsic microglia, the infiltration of monocytes into gliomas to become macrophages makes it important to address the roles of these blood-derived cells. We found no evidence of functional separation of microglia from monocytes and macrophages, as all of these monocytoid populations exerted an equivalent capacity to reduce BTIC sphere formation in culture (Fig. 1). The fact that AmpB enters the CNS makes it attractive as a therapeutic for BTICs, as not only would blood-borne cells be mobilized, but the microglia around gliomas would also be activated.

Our finding that AmpB has the potential to treat gliomas is supported by a case report³⁵ of an 11-year-old child with Grade III astrocytoma who appeared terminal 6 weeks following diagnosis. The patient developed fungal infections and was treated with AmpB for 3 months; the patient went into apparent remission from her glioma and, at the time of the report (8 months), had improved clinically.

TLR ligands such as the classic TLR4 stimulator, bacterial LPS, may be used to activate monocytoid cells, but their utility as therapeutics is questionable because of safety issues. We developed AmpB as a potential therapeutic for gliomas based on its identification among 1,040 medications that further activated LPS-stimulated microglia in culture. AmpB has already been shown to activate macrophages in culture^{36,37}, which validates our screening process. Nonetheless, the potential for AmpB to activate innate immunity and suppress BTICs is unknown, and our current results provide a new approach to glioma therapy.

As an anti-fungal medication, AmpB acts by binding to sterols in the cell membrane of susceptible fungi to alter membrane permeability and induce the leakage of intracellular content. AmpB treatment, however, can have substantial toxicity, which occurs at serum concentrations of 500–2,000 ng ml⁻¹ in humans. We did not encounter toxicity with chronic daily injections of AmpB in mice, likely as a result of the low dose that we employed, with observed serum concentration of 56 ng ml⁻¹ 2 h after 30 injections. This differential and safety margin is helpful to guide the potential use of AmpB in patients with gliomas. Clearly, any trials in human gliomas will have to involve a dose-ranging study.

The microglia cells are sensors of pathology in the CNS, whereas macrophages are recruited to the CNS following injury; both cell types of different lineages participate in the defense against insults through multiple mechanisms^{38,39}. Our results suggest the involvement

of microglia-derived IL-8 and MCP-1 in the reduction of BTIC sphere formation (Fig. 3). Other molecules may also be involved, and this is indicated by the capacity of TNF- α to reduce BTIC growth. Finally, we do not know if there is an interaction between IL-8 and MCP-1, or if BTICs would also be producing these chemokines for auto-crine or paracrine growth following encounter with microglia; in isolation, BTICs did not express detectable levels of IL-8 or MCP-1 (Supplementary Fig. 3). Clearly, the roles of IL-8 and MCP-1 from activated macrophages and microglia would need to be addressed in the future. It is noteworthy that glioma-derived microglia produced low levels of IL-8 and MCP-1 until stimulated by AmpB, which restored their capacity to reduce BTIC growth.

Our results highlight the microenvironment around tumors, particularly the representation of immune cells, as a regulator of malignancy. One such population, tumor-associated macrophages (and microglia in the CNS), is thought initially to infiltrate into tumors to eradicate transformed cells, but they often become immunosuppressed in tumors⁴⁰. Indeed, immune cells are thought to be coerced to promote tumorigenicity^{41–43}. In this regard, immunity in patients with malignant gliomas is generally considered to be compromised, with the tumor cell deactivating immune cell subsets that seek to eradicate it, or with the tumor exploiting immune cells for growth and invasiveness^{9–13}; this compromise was noted in our experiments, as the glioma-derived microglia were unable to reduce BTIC growth, likely as a result of chronic *in vivo* exposure to the molecules produced by tumors to inhibit immunity, including TGF- β , IL-10 and several prostanoids. In this light, our results indicate that CNS monocytoid cells can be stimulated with an available medication, AmpB, to sway the balance of immunity toward curbing BTICs. Finally, our results are relevant to other tumors, in which it may be possible to use AmpB to activate monocytoid cells to overcome tumor-induced suppressive microenvironment and curb tumorigenicity.

METHODS

Methods and any associated references are available in the [online version of the paper](#).

Accession codes. All microarray data has been submitted to the US National Institute of Health GEO database under accession number GSE52127.

Note: Any Supplementary Information and Source Data files are available in the online version of the paper.

ACKNOWLEDGMENTS

We acknowledge the technical assistance of Y. Fan, X. Zhang, F. Yong, J. Wang, H. Mowbray, B. Verhaeghe, M. Keough, R. Hassam, B. McKenzie and A. Luchman. Clodronate was a gift from Roche Diagnostics GmbH. We thank Alberta Innovates – Health Solutions/Alberta Cancer Foundation and the Canadian Institutes of Health Research for operating grant support. V.W.Y. is a Canada Research Chair (Tier 1) in Neuroimmunology, for which salary support is gratefully acknowledged.

AUTHOR CONTRIBUTIONS

S.S. designed all of the experiments, conducted and analyzed the data from the majority of the experiments, supervised the acquisition of all datasets, and wrote and edited the manuscript. A.D. performed the PCR analyses, conducted the liposome treatment of mice and edited the manuscript. E.J.Z. transfected GL261 with luciferase reporter, performed bioluminescence imaging and analyses, and guided aspects of the study. C.S. helped process the cells from tumor specimens and conducted some of the experiments. X.L. implanted mice with intracranial human BTICs, cross-checked the *in vivo* datasets and edited the manuscript. X.W. performed the microarray experiments and analyses. J.K. was instrumental in the derivation of BTIC lines from resected human specimens and in the analyses of the genetic alterations of the cells, and edited the manuscript. W.H. provided the surgically resected brain materials from epilepsy cases from which

non-transformed adult human microglia were derived and edited the manuscript. M.H. provided the resected glioblastoma and blood specimens from which BTICs, tumor-derived microglia and monocytes were obtained and edited the manuscript. P.M. provided the resected glioblastoma and blood specimens from which BTICs, tumor-derived microglia and monocytes were obtained and edited the manuscript. J.F.D. performed the MRI studies, adapted human imaging to evaluation in mice and edited the manuscript. D.K. supervised the measurements of levels of AmpB in mice. N.V.R. supplied the clodronate liposomes and advised on its use. S.R. supervised the microarray analyses and edited the manuscript. P.F. provided expertise with regards to the implantation of BTICs in mice and the treatment procedures of mice with intracranial tumors and edited the manuscript. G.C. supervised the BTIC bank that houses the patient-derived lines used in this study, provided general expertise on brain tumors and edited the manuscript. S.W. co-supervised the BTIC bank, provided expertise on stem cells and edited the manuscript. V.W.Y. supervised all aspects of this work, designed the majority of experiments, obtained the funding for this study and edited the manuscript.

COMPETING FINANCIAL INTERESTS

The authors declare no competing financial interests.

- Singh, S.K. *et al.* Identification of human brain tumour initiating cells. *Nature* **432**, 396–401 (2004).
- Kelly, J.J. *et al.* Proliferation of human glioblastoma stem cells occurs independently of exogenous mitogens. *Stem Cells* **27**, 1722–1733 (2009).
- Bao, S. *et al.* Glioma stem cells promote radioresistance by preferential activation of the DNA damage response. *Nature* **444**, 756–760 (2006).
- Eramo, A. *et al.* Chemotherapy resistance of glioblastoma stem cells. *Cell Death Differ.* **13**, 1238–1241 (2006).
- Chen, J. *et al.* A restricted cell population propagates glioblastoma growth after chemotherapy. *Nature* **488**, 522–526 (2012).
- Cheng, L., Bao, S. & Rich, J.N. Potential therapeutic implications of cancer stem cells in glioblastoma. *Biochem. Pharmacol.* **80**, 654–665 (2010).
- Dietrich, J., Diamond, E.L. & Kesari, S. Glioma stem cell signaling: therapeutic opportunities and challenges. *Expert Rev. Anticancer Ther.* **10**, 709–722 (2010).
- Charles, N.A., Holland, E.C., Gilbertson, R., Glass, R. & Kettenmann, H. The brain tumor microenvironment. *Glia* **60**, 502–514 (2012).
- Yang, I., Han, S.J., Kaur, G., Crane, C. & Parsa, A.T. The role of microglia in central nervous system immunity and glioma immunology. *J. Clin. Neurosci.* **17**, 6–10 (2010).
- Hussain, S.F. *et al.* The role of human glioma-infiltrating microglia/macrophages in mediating antitumor immune responses. *Neuro-oncol.* **8**, 261–279 (2006).
- Kerber, M. *et al.* Flt-1 signaling in macrophages promotes glioma growth in vivo. *Cancer Res.* **68**, 7342–7351 (2008).
- Markovic, D.S. *et al.* Gliomas induce and exploit microglial MT1-MMP expression for tumor expansion. *Proc. Natl. Acad. Sci. USA* **106**, 12530–12535 (2009).
- Bettinger, I., Thanos, S. & Paulus, W. Microglia promote glioma migration. *Acta Neuropathol.* **103**, 351–355 (2002).
- Hwang, S.Y. *et al.* Induction of glioma apoptosis by microglia-secreted molecules: the role of nitric oxide and cathepsin B. *Biochim. Biophys. Acta* **1793**, 1656–1668 (2009).
- Mora, R. *et al.* TNF-alpha- and TRAIL-resistant glioma cells undergo autophagy-dependent cell death induced by activated microglia. *Glia* **57**, 561–581 (2009).
- Brantley, E.C. *et al.* Nitric oxide-mediated tumoricidal activity of murine microglial cells. *Transl. Oncol.* **3**, 380–388 (2010).
- Kees, T. *et al.* Microglia isolated from patients with glioma gain antitumor activities on poly (I:C) stimulation. *Neuro-oncol.* **14**, 64–78 (2012).
- Chicoine, M.R. *et al.* The *in vivo* antitumoral effects of lipopolysaccharide against glioblastoma multiforme are mediated in part by Toll-like receptor 4. *Neurosurgery* **60**, 372–380 (2007).
- Galarneau, H., Villeneuve, J., Gowing, G., Julien, J.P. & Vallieres, L. Increased glioma growth in mice depleted of macrophages. *Cancer Res.* **67**, 8874–8881 (2007).
- Wu, A. *et al.* Glioma cancer stem cells induce immunosuppressive macrophages/microglia. *Neuro-oncol.* **12**, 1113–1125 (2010).
- Ye, X.Z. *et al.* Tumor-associated microglia/macrophages enhance the invasion of glioma stem-like cells via TGF- β 1 signaling pathway. *J. Immunol.* **189**, 444–453 (2012).
- Williams, K. *et al.* Biology of adult human microglia in culture: comparisons with peripheral blood monocytes and astrocytes. *J. Neuropathol. Exp. Neurol.* **51**, 538–549 (1992).
- Giuliani, F., Hader, W. & Yong, V.W. Minocycline attenuates T cell and microglia activity to impair cytokine production in T cell-microglia interaction. *J. Leukoc. Biol.* **78**, 135–143 (2005).
- Brescia, P. *et al.* CD133 is essential for glioblastoma stem cell maintenance. *Stem Cells* **31**, 857–869 (2013).
- Hu, Y. & Smyth, G.K. ELDA: extreme limiting dilution analysis for comparing depleted and enriched populations in stem cell and other assays. *J. Immunol. Methods* **347**, 70–78 (2009).
- Zheng, H. *et al.* p53 and Pten control neural and glioma stem/progenitor cell renewal and differentiation. *Nature* **455**, 1129–1133 (2008).
- Lawrence, D.M. *et al.* Astrocyte differentiation selectively upregulates CCL2/monocyte chemoattractant protein-1 in cultured human brain-derived progenitor cells. *Glia* **53**, 81–91 (2006).
- Edman, L.C. *et al.* Alpha-chemokines regulate proliferation, neurogenesis, and dopaminergic differentiation of ventral midbrain precursors and neurospheres. *Stem Cells* **26**, 1891–1900 (2008).
- Samanani, S. *et al.* Screening for inhibitors of microglia to reduce neuroinflammation. *CNS Neurol. Disord. Drug Targets* **12**, 741–749 (2013).
- Tang, X., Mo, C., Wang, Y., Wei, D. & Xiao, H. Anti-tumour strategies aiming to target tumour-associated macrophages. *Immunology* **138**, 93–104 (2013).
- Popovich, P.G. *et al.* Depletion of hematogenous macrophages promotes partial hindlimb recovery and neuroanatomical repair after experimental spinal cord injury. *Exp. Neurol.* **158**, 351–365 (1999).
- Polfliet, M.M. *et al.* A method for the selective depletion of perivascular and meningeal macrophages in the central nervous system. *J. Neuroimmunol.* **116**, 188–195 (2001).
- Wu, A. *et al.* Persistence of CD133+ cells in human and mouse glioma cell lines: detailed characterization of GL261 glioma cells with cancer stem cell-like properties. *Stem Cells Dev.* **17**, 173–184 (2008).
- Bertrand, J. *et al.* Cancer stem cells from human glioma cell line are resistant to Fas-induced apoptosis. *Int. J. Oncol.* **34**, 717–727 (2009).
- Rubissow, M.J. Remission of astrocytoma following amphotericin-B treatment. *Lancet* **1**, 565 (1970).
- Tokuda, Y. *et al.* Augmentation of murine tumor necrosis factor production by amphotericin B *in vitro* and *in vivo*. *Antimicrob. Agents Chemother.* **37**, 2228–2230 (1993).
- Wilson, E., Thorson, L. & Speert, D.P. Enhancement of macrophage superoxide anion production by amphotericin B. *Antimicrob. Agents Chemother.* **35**, 796–800 (1991).
- Neumann, H. & Wekerle, H. Brain microglia: watchdogs with pedigree. *Nat. Neurosci.* **16**, 253–255 (2013).
- Hanisch, U.K. & Kettenmann, H. Microglia: active sensor and versatile effector cells in the normal and pathologic brain. *Nat. Neurosci.* **10**, 1387–1394 (2007).
- Allavena, P., Sica, A., Garlanda, C. & Mantovani, A. The Yin-Yang of tumor-associated macrophages in neoplastic progression and immune surveillance. *Immunol. Rev.* **222**, 155–161 (2008).
- Mantovani, A., Allavena, P., Sica, A. & Balkwill, F. Cancer-related inflammation. *Nature* **454**, 436–444 (2008).
- Qian, B.Z. & Pollard, J.W. Macrophage diversity enhances tumor progression and metastasis. *Cell* **141**, 39–51 (2010).
- Galvão, R.P. & Zong, H. Inflammation and gliomagenesis: bi-directional communication at early and late stages of tumor progression. *Curr. Pathobiol. Rep.* **1**, 19–28 (2013).

ONLINE METHODS

Human BTICs. The generation of primary BTIC lines from resected specimens of patients with malignant gliomas was described previously². A number of the described lines were used here: 25EF, 48EF, 69EF and 53M. We also cultured microglia and BTICs from the same glioblastoma subjects and designated these as GBM1–6. To propagate the BTIC lines in perpetuity, cells were dissociated and plated into T25 flasks at regular intervals and grown in serum-free culture medium supplemented with EGF and FGF-2, as described previously²; the exception was 53M, which was grown in the same medium, but without added growth factors, as the latter cause 53M to become a monolayer. Cultures were fed weekly by removing half of the existing medium and replacing with an equal volume of fresh medium. In such conditions, the BTIC lines grew in progressively enlarging spheres. All experiments with human cells or resected brain specimens were conducted with approval from the Conjoint Health Research Ethics Board, University of Calgary, with informed consent from the human subjects.

BTIC-microglia co-culture experiments. Microglia were cultured from adult²² or fetal²³ human brains and from resected glioblastoma patients, as approved by the Conjoint Health Research Ethics Board, University of Calgary. Informed consent was obtained from all patients. Cells (10,000 cells per well per 100 μ l of MEM supplemented with 10% FBS, vol/vol) were plated into 96-well plates. During the course of experiments, microglia and all other cell types were switched to the serum-free BTIC medium. For co-culture experiments, medium was removed from microglia and dissociated cells from BTIC spheres were added at a density of 10,000 cells per 100 μ l of serum-free BTIC medium. The plate was kept at 37 °C in 5% CO₂ incubator. After 72 h, four random fields per well were photographed under a 10 \times objective in a phase-contrast microscope, and the number of spheres over 60 μ m in diameter was tabulated. In selected experiments, the BTICs and microglia were separated by a 0.4- μ m pore-size filter to prevent cell-cell contact, and the number of spheres over 60 μ m in four fields was determined. Finally, BTICs were exposed to conditioned medium from different cell types, including peripheral blood human monocytes, human microglia, neurons and astrocytes; neural cells were isolated and cultured as previously described⁴⁴. Monocytes were isolated from human peripheral blood mononuclear cells using CD14⁺ magnetic beads (Stem Cell Technology), and maintained in RPMI medium supplemented with 20% human serum (vol/vol). Macrophages were derived from isolated CD14⁺ monocytes by culturing them in RPMI medium with M-CSF (10 ng ml⁻¹) for 7 d.

Treatment of BTIC cultures with function-blocking antibodies and siRNA. BTICs were plated in a 96-well plate (10,000 BTICs per 100 μ l of medium) for 72 h. Cells were treated with or without IL-8 (10 ng ml⁻¹) or MCP-1 (10 ng ml⁻¹) either singly or in combination. In a different set of experiment, cells were treated with MCM either in presence or absence of function blocking antibodies to IL-8 (ab10769, Abcam) or MCP-1 (ab9669, Abcam) (10 μ g ml⁻¹) or isotype control antibody (ab37388, Abcam) and number of spheres was quantified after 72 h.

For siRNA to CCR2, a silencer select pre-designed siRNA (21 oligonucleotides in length, Ambion) was used to target human CCR2. The sequence was 5'-GGC UGU AUC ACA UCG GUU Att-3'. A second siRNA, designated CCR2 siRNA2 was used to confirm the CCR2 siRNA1 result. The sequence of siRNA2 was 5'-CGG UGC UCC CUG UCA UAA Att-3.

For transfection with siRNA⁴⁵, BTICs were plated in 12-well plates and were incubated with 5 nM siRNA and lipofectamine (Invitrogen). After 24 h, cells were harvested and exposed to MCM and number of spheres was quantified after 72 h.

Immunofluorescence. BTIC spheres were grown in a 96-well plate and cultured with or without MCM or AmpB/MCM. In some experiments, such as for characterization, spheres were spun down to the bottom of wells using cytospin, and were fixed with 4% paraformaldehyde (vol/vol). 0.02% Triton X-100 (vol/vol) in PBS was then added to permeabilize cells. Wells were blocked for nonspecific binding overnight at 4 °C. Spheres or adherent cells were incubated with primary antibodies: rabbit antibody to GFAP (1:200, Z0334, Dakocytomation), mouse antibody to β III tubulin (1:200, MAB1637, Chemicon), mouse antibody to human nestin (1:200, MAB5326, Millipore), rabbit antibody to Sox2 (1:200, AB5603, Millipore), Musashi-1 (1:200, AB5977, Millipore) and rabbit antibody to ID4 (1:200, SCI13047, Santa Cruz Biotechnology). Following washes, cells

or spheres were incubated with an Alexa 488- (mouse, 1:500, A11001; rabbit, 1:500, A11008; Molecular Probes, Invitrogen) or Cy3-conjugated (1:500, 115-166-003, Jackson ImmunoResearch) secondary antibodies for 1 h. Cells were counterstained with nuclear yellow for 30 min at 22 °C. The proportion of cells per well expressing markers of interest was quantified using an epifluorescence microscope built into the ImageXpress^{MICRO} (IXM, Molecular Devices), a high-throughput cellular imaging system. Images from 96-well plates were acquired on the IXM, which consists of imaging hardware controlled by MetaXpress, the image analysis software.

Microarray and data analysis. RNA was extracted using the mirVana miRNA Isolation Kit (Ambion) according to the manufacturer's protocol. Total RNA was purified with the RNeasy Plus Micro Kit (Qiagen) to remove genomic DNA. The RNA quality of integrity number (RIN) was measured with an Agilent RNA 6000 NanoChip on 2100 Bioanalyzer (Agilent Technologies). The quantity was measured with NanoDrop 1000 (NanoDrop Technologies). 100 μ g of RNA of each sample with a RIN higher than 9 was labeled with the 3' IVT Express Kit (Ambion) and hybridized to an Affymetrix GeneChip Human Genome U133 Plus 2.0 Array at 45 °C for 16 h. Arrays were stained and washed on an Affymetrix GeneChip Fluidics 450 following manufacturer's protocol and scanned with an Affymetrix GeneChip Scanner 3000 7G System. Array data files were generated with GeneChip Command Console Software (AGCC) and statistical significant analysis was carried out on software of GeneSpring (Agilent Technologies). The fold change between treatment and control was based on the $P < 0.05$ from unpaired t test (Asymptotic and Benjamini Hochberg FDR).

Quantitative real-time PCR. Cells were lysed in 300 μ l TRIzol reagent (Invitrogen) by leaving plates at 22 °C for 5 min before the content of the well was harvested and stored at -80 °C before use. Following extraction (Qiagen), RNA was first treated with DNase (Promega) and reverse transcribed using Superscript II reverse transcriptase (Invitrogen). The resulting cDNA was used as a template for the BioRad iCycler MyiQ detection system and 2 \times SYBR green mastermix (Qiagen). Every primer (10 \times QuantiTect Primer Assay) that was used was purchased from Qiagen. Expression of gene transcripts was normalized against at least two housekeeping genes, *GAPDH* and *ACTB*. Relative expression levels for our genes of interest was determined using the formula 2- Δ CT where Δ CT = CT (gene of interest) - CT (housekeeping gene).

Western blot analysis. BTIC cells (25EF, 48EF) were exposed to MCM for 6 h, and cell lysates were prepared using lysis buffer on ice and total protein was measured as described previously⁴⁵. Equal amounts of proteins were electrophoresed on 10% Bis-Tris gels under reducing conditions and transferred to a polyvinylidene difluoride membrane (Millipore). The latter was then blocked for 2 h with 5% milk (wt/vol) in saline and was then probed overnight with rabbit antibody to human Thbs1 (1:1,000, ab85762, Abcam) or rabbit antibody to human Jak1 (1:1,000, 3332, Cell Signaling). A secondary antibody to rabbit horseradish peroxidase (1:5,000–10,000) was added for 1 h, and signals were detected by enhanced chemiluminescence detection kit (Amersham Bioscience).

ELISA and luminex analyses. The activity of microglia was evaluated by ELISA of the conditioned medium of cells growing in 96-well plate. We routinely measure TNF- α , as this is a reliable, robust and easily measurable molecule produced by microglia following their activation. To analyze the content of conditioned media simultaneously for multiple cytokines and chemokines, a multiplex analysis (Eves) of the above conditioned medium was used.

Cell cycle analysis, Annexin V-propidium iodide staining and FACS analysis. BTIC cells were treated with or without MCM for 72 h, and cell cycle analysis was performed with propidium iodide using standard flow cytometry protocol⁴⁶. Similarly, BTICs were cultured with or without MCM for 72 h and then cells were stained using an Annexin V-propidium iodide staining kit to determine apoptotic or necrotic cells. CD133 and CCR2 expression was also determined using a standard flow cytometry protocol.

BrdU staining. BTIC (25EF) (5,000 per 100 μ l) were plated in each well of a 16-well lab tek chamber slide and treated with or without MCM. After 48 h, 10 μ M BrdU was added to the medium, incubated for 2 h and washed with PBS

three times. Cells were fixed with methanol (10%, vol/vol) for 10 min at 4 °C and incubated in 1 N HCl for 30 min at 22 °C. Cells were then washed with PBS and incubated with 0.1 M sodium tetraborate for 15 min and washed again with PBS. Cells were next incubated with mouse antibody to BrdU (MA3-071, Thermo Scientific, diluted 1:100 in 10% goat serum and 2% horse serum in Hank's balanced salt solution, HHG) overnight at 4 °C, followed by goat antibody to mouse Cy3 (115-166-003, Jackson ImmunoResearch, diluted 1:200 in HHG) for 1 h and finally counter stained with nuclear yellow for 10 min and quantified under a fluorescence microscope.

Mice, BTIC implantation, treatment with AmpB and monitoring. BTIC spheres from 25EF and 48EF lines or CD133⁺ cells from the GL261 line were mechanically dissociated into single-cell suspensions. Cells were washed with BTIC medium. 10,000 viable cells were resuspended in 2 µl of PBS and implanted into the right striatum of 6–8-week-old female NOD-SCID mice or C57BL/6 mice (Charles River, Montreal) stereotactically². Mice were kept in a vivarium (normally five per cage) with regular light/dark cycles. Mice were treated with AmpB (fungizone[®], from GIBCO Invitrogen) 7 d later at a dose of 0.2 mg per kg per d (intraperitoneal) until the termination of the experiment. Fungizone is AmpB solubilized into a colloidal dispersion with sodium deoxycholate, and buffered with sodium phosphates; this mixture is similar to that used to medicate patients with severe fungal infections. Thus, control mice were injected with an identical vehicle solution. In initial dose-testing experiments, we determined that mice appeared normal after prolonged (1 month) daily intraperitoneal treatment with 0.2 and 1 mg per kg AmpB. In all cases, mice were randomized into cages that were then assigned particular treatments. When LPS was administered, this was given at 1 mg per kg intraperitoneal at weekly intervals following a protocol that results in activation of microglia in the CNS⁴⁷.

At days 49 or 70 post-implantation, MRI of brain was conducted at the University of Calgary Experimental Imaging Center as previously described² using a 9.4-T Bruker horizontal-bore MR system. Images were analyzed using Marevici software. For bioluminescence studies, mice were imaged with the Xenogen IVIS 200 system (Xenogen). Data were analyzed based on total photon flux emission (photons per s) in the region of interest⁴⁸.

As a major outcome of the mouse study was whether AmpB could prolong the life of mice with intracranial human BTICs, we continued daily intraperitoneal injections of AmpB or vehicle until the mice died. We used Kaplan-Meier survival curves in which mice found dead in their cages were recorded; in most cases, however, and in accordance with ethical guidelines, mice that were moribund (negligible limb movement, and loss of 25% of body weight from the preceding few days) were considered to be dead and were killed. Evaluators were not blinded as to the treatment groups, and evaluations were conducted during the day. All protocols were approved by the Animal Care Committee at the University of Calgary in accordance with research guidelines from the Canadian Council for Animal Care.

Implantation of BTIC exposed to various conditioned media. In a different set of experiments, BTICs were exposed to microglia conditioned medium (MCM) or conditioned medium from AmpB-treated (1 µM) microglia (Amp/MCM) and then implanted into the brain of NOD/SCID mice as described before. For the generation of MCM, 2,000,000 human adult microglia cells were incubated for 48 h with 1 ml of serum-free BTIC medium supplemented with EGF or FGF in a 6-well plate in a 5% CO₂ incubator. For AmpB/MCM, microglia cells were plated similarly but were treated with 1 µM of AmpB. The conditioned medium was collected after 48 h. Finally, before implantation, BTICs were exposed to MCM or AmpB/MCM in a 96-well plate (10,000 BTICs per 100 µl of medium) for 72 h. In other wells, BTICs were treated with 1 µM AmpB or vehicle for 72 h, in the absence of microglia. Cells were then dissociated to produce single-cell suspensions of BTICs for implantation into the brain of NOD-SCID mice.

Histological and immunohistochemical analyses of intracranial tumor. To assess tumor size and spread in asymptomatic mice, mice were killed 49 days after implantation and processed as previously described vol/vol⁴⁹. The whole brain was removed, cut into blocks, fixed in 10% buffered formalin (vol/vol) and embedded in paraffin. Sections of 6 µm were taken every 120 µm apart, through the entire brain. The sections were deparaffinized, rehydrated and stained with hematoxylin and eosin. All sections were analyzed for the presence of tumor growth through detection of areas of hypercellularity; by documenting how many sections spaced 120 µm apart per brain contained tumor, the spread of tumor across the entire rostral caudal extent of the brain could thus be determined. The section containing the largest tumor mass was subjected to area analysis of the tumor using ImageJ software. As sections were spaced 120 µm apart, this was calculated to obtain the tumor volume.

For immunostainings, deparaffinized sections were subjected to endogenous peroxidase inactivation using 1% H₂O₂ (vol/vol) in methanol. The sections were incubated with 4% horse serum to block nonspecific binding, then incubated with rabbit antibody to Iba1 to detect microglia and macrophage (1:500, 019-19741, WAKO), rabbit antibody to inducible nitric oxide synthase (iNOS, 1:50, 610333, Becton Dickinson) to detect the pro-inflammatory nature of macrophages and microglia, or rabbit antibody to Ki67 (1:1,000, Leica Microsystems) for proliferation index. Incubation occurred overnight at 4 °C, followed successively by the biotinylated secondary antibody, ABC reagent (Vectastain ABC kit, Vector Laboratories) and diaminobenzidine. The slides were then lightly counterstained with hematoxylin, dehydrated and mounted.

Iba1⁺ cells were quantified by counting golden-brown cells from five different fields of a section adjacent to the one identified by hematoxylin and eosin to contain the largest tumor mass. The five fields consisted of one from the center of the tumor core, one each midway between the core and the top and bottom boundaries of the tumor, and one each midway between the core and the left and right extent of the tumor. In other experiments, the density of Iba1 or iNOS-positive profiles was quantified by ImageJ analyses.

Statistical analyses. Kaplan-Meier survival curves were analyzed for statistical difference between groups using the log-rank test. For analyses of differences in sphere formation in culture, the one-way ANOVA with *post hoc* Tukey's comparisons was used for multiple groups, whereas the two-sided unpaired *t* test was used for comparisons of two groups. No statistical methods were used to pre-determine sample sizes, but our sample size per experiment was based on successes in prior experiments with cells in culture or in groups of mice to discern an effect^{2,3,26,45}. Data distribution was assumed to be normal, but this was not formally tested. Data collection and analysis were not performed blind to the conditions of the experiments. Unless otherwise stated, all experiments were reproduced at least twice.

44. Vecil, G.G. *et al.* Interleukin-1 is a key regulator of matrix metalloproteinase-9 expression in human neurons in culture and following mouse brain trauma *in vivo*. *J. Neurosci. Res.* **61**, 212–224 (2000).
45. Sarkar, S., Nuttall, R.K., Liu, S., Edwards, D.R. & Yong, V.W. Tenascin-C stimulates glioma cell invasion through matrix metalloproteinase-12. *Cancer Res.* **66**, 11771–11780 (2006).
46. Besson, A. & Yong, V.W. Involvement of p21(Waf1/Cip1) in protein kinase C alpha-induced cell cycle progression. *Mol. Cell Biol.* **20**, 4580–4590 (2000).
47. Nguyen, M.D., D'Aigle, T., Gowing, G., Julien, J.P. & Rivest, S. Exacerbation of motor neuron disease by chronic stimulation of innate immunity in a mouse model of amyotrophic lateral sclerosis. *J. Neurosci.* **24**, 1340–1349 (2004).
48. Lun, X. *et al.* Efficacy and safety/toxicity study of recombinant vaccinia virus JX-594 in two immunocompetent animal models of glioma. *Mol. Ther.* **18**, 1927–1936 (2010).
49. Zhou, Y. *et al.* The chemokine GRO-alpha (CXCL1) confers increased tumorigenicity to glioma cells. *Carcinogenesis* **26**, 2058–2068 (2005).